Electronic supplementary materials *Mendeleev Commun.*, 2025, **35**, 676–680

Slow relaxation of magnetization and luminescence in seven- and six-coordinate Tb^{3+} complexes

Dmitry M. Lyubov, Gautier Félix, Aleksey O. Tolpygin, Tatyana V. Mahrova, Yulia V. Nelyubina, Saad Sene, Vladislav M. Korshunov, Ilya V. Taydakov, Andrey A. Tyutyunov, Boris Le Guennic, Olivier Cador, Yannick Guari, Joulia Larionova and Alexander A. Trifonov

Table of Contents

Experimental section

General Procedure

All experiments were conducted in an argon atmosphere using Schlenk techniques or within a nitrogen-filled glovebox. THF was first dried over KOH and then purified by distillation over sodium/benzophenone ketyl. Hexane was dried using Na/K alloy, transferred under vacuum, and stored in the glovebox. Fluorinated alcohols $HOCH(CF_3)Ph$, $HOC_6F_4C_6F_5$, $HOC(CF_3)_2Ph$, and $HOC(CF_3)_3$ were purchased from SIA "P&M-Invest" Ltd, were dried over molecular sieves, then condensed in vacuum prior to use. $TbCl_3$,[S1] o-Me_2N-$C_6H_4CH_2Li$ [S2] and $[HNEt_3][BPh_4]_2$ [S3] were synthesized according to the literature procedures. IR spectra were recorded as Nujol mulls on a Bruker-Vertex 70 spectrophotometer. The C, H, N elemental analyses were carried out in the microanalytical laboratory of IOMC by means of a Carlo Erba Model 1106 elemental analyzer with an accepted tolerance of 0.4 unit on carbon (C), hydrogen (H), and nitrogen (N). Lanthanide analysis was carried out by complexometric titration.[S4] IR spectra were recorded as Nujol mulls on a Bruker-Vertex 70 spectrophotometer.

Synthesis of $Tb(CH_2C_6H_4NMe_2\text{-}o)_3$: A solution of *o*-$Me_2NC_6H_4CH_2Li$ (2.39 g, 16.9 mmol) in 20 mL of THF was added to a suspension of $TbCl_3$ (1.50 g, 5.65 mmol) in 20 mL of THF at −30 °C. The reaction mixture was slowly warmed to ambient temperature and additionally was stirred for 1 hour. All the volatiles were removed in vacuum. The solid residue was dissolved in toluene (50 mL) and filtered. The solution was concentrated to 10 mL. Prolonged cooling of toluene solution at −30 °C led to orange crystals of $Tb(CH_2C_6H_4NMe_2\text{-}o)_3$ which was isolated in 66% yield (2.09 g). Elemental analysis calc. for $C_{27}H_{36}N_3Tb$ (561.52 g·mol^{-1}) (%): C, 57.75; H, 6.46; N, 7.48; Tb, 28.30. Found (%): C, 57.91; H, 6.67; N, 7.21; Tb, 28.21. IR (Nujol, KBr) ν/cm^{-1}: 1586 (s), 1548 (s), 1405 (m), 1299 (s), 1273 (s), 1259 (s), 1227 (s), 1170 (s), 1155 (s), 1147 (m), 1103 (s), 1046 (s), 1029 (s), 1021 (s), 985 (w), 967 (w), 961 (w), 930 (s), 920 (s), 845 (s), 822 (s), 760 (s), 743 (s), 588 (s), 562 (m), 523 (s), 497 (s), 485 (w), 474 (m) (Figure S1, ESI).

Synthesis of $[Tb(OCH(CF_3)Ph)_2(THF)_5][BPh_4]$ (1): A THF solution (10 mL) of $[HNEt_3][BPh_4]$ (0.26 g, 0.62 mmol) was added to a solution of $Tb(CH_2C_6H_4NMe_2\text{-}o)_3$ (0.36 g, 0.64 mmol) in THF (10 mL) at ambient temperature. The solution was stirred for 30 min and then $HOCH(CF_3)Ph$ (0.23 g, 1.30 mmol) was added and the reaction mixture was stirred additionally for 30 min. The volatiles were removed in vacuum; the oily residue was dried in vacuum at 50 °C for 30 min and was dissolved in fresh portion of THF (approx. 10 mL). Complex 1 was isolated by slow diffusion of hexane into THF solution (1:1 ratio) at ambient temperature as colourless crystals. in 75 % yield (0.57 g). Elemental analysis calc. for $C_{60}H_{72}BF_6O_7Tb$ (1188.94 g·mol^{-1}) (%): C, 60.61; H, 6.10; Tb, 13.37. Found (%): C, 60.83; H, 6.33; Tb, 13.19. IR (Nujol, KBr) ν/cm^{-1}: 1950 (m), 1890 (m), 1820 (m), 1770 (w), 1680 (m), 1650 (m), 1615 (s), 1580 (s), 1495 (s), 1480 (s), 1430 (s), 1260 (s), 1205 (m), 1160 (s), 1120 (s), 1065 (m), 1030 (s), 920

(m), 870 (s), 840 (m), 765 (m), 735 (s), 705 (s), 675 (w), 635 (m), 610 (s), 585 (m), 530 (w), 470 (m) (Figure S2, ESI).

Synthesis of [Tb(OC$_6$F$_4$C$_6$F$_5$)$_2$(THF)$_5$][BPh$_4$] (2): Complex 2 was synthesized and isolated analogously to **1**, starting from Tb(CH$_2$C$_6$H$_4$NMe$_2$-*o*)$_3$ (0.330 g, 0.59 mmol), [HNEt$_3$][BPh$_4$] (0.245 g, 0.58 mmol), and HOC$_6$F$_4$C$_6$F$_5$ (0.395 g, 1.19 mmol mmol). Complex **2** was isolated as colorless crystals in 79% yield (0.730 g). Elemental analysis calc. for C$_{68}$H$_{60}$BF$_{18}$O$_7$Tb·(C$_4$H$_8$O) (1573.01 g·mol^{-1}) (%): C, 54.98; H, 4.36; Tb, 10.10. Found (%): C, 54.84; H, 4.40; Tb, 9.97. IR (Nujol, KBr) ν/cm^{-1}: 1945 (m), 1880 (m), 1820 (m), 1760 (w), 1685 (w), 1650 (s), 1610 (m), 1580 (m), 1505 (s), 1490 (m), 1430 (m), 1260 (s), 1170 (s), 1090 (s), 1020 (m), 995 (m), 970 (s), 920 (m), 860 (s), 805 (m), 705 (s), 670 (w), 645 (s), 610 (s), 580 (m), 475 (s) (Figure S3, ESI).

Synthesis of [Tb(OC(CF$_3$)$_2$Ph)$_2$(THF)$_4$][BPh$_4$] (3): Complex **3** was synthesized and isolated analogously to **1**, starting from Tb(CH$_2$C$_6$H$_4$NMe$_2$-*o*)$_3$ (0.355 g, 0.63 mmol), [HNEt$_3$][BPh$_4$] (0.260 g, 0.62 mmol), and HOC(CF$_3$)$_2$Ph (0.310 g, 1.27 mmol). Complex **3** was isolated as colorless crystals in 69% yield (0.545 g). Elemental analysis calc. for C$_{58}$H$_{62}$BF$_{12}$O$_6$Tb (1252.83 g·mol^{-1}) (%): C, 55.60; H, 4.99; Tb, 12.69. Found (%): C, 55.67; H, 4.81; Tb, 12.44. IR (Nujol, KBr) ν/cm^{-1}: 1960 (w), 1940 (m), 1880 (m), 1815 (m), 1760 (w), 1680 (s), 1605 (m), 1580 (s), 1560 (w), 1500 (m), 1425 (s), 1345 (w), 1295 (m), 1270 (s), 1210 (s), 1195 (s), 1145 (s), 1080 (m), 1035 (m), 1005 (s), 965 (s), 940 (s), 915 (m), 850 (s), 770 (s), 745 (m), 705 (s), 670 (w), 660 (m), 625 (w), 610 (s), 560 (m), 535 9m), 520 (m), 500 (m), 470 (m) (Figure S4, ESI).

Synthesis of [Tb(OC(CF$_3$)$_3$)$_3$(THF)$_3$] (4): Protocol A: A synthetic approach analogous to the one used for **1**, starting from Tb(CH$_2$C$_6$H$_4$NMe$_2$-*o*)$_3$ (0.370 g, 0.66 mmol), [HNEt$_3$][BPh$_4$] (0.277 g, 0.66 mmol), and HOC(CF$_3$)$_3$ (0.311 g, 1.32 mmol, 1.83 mL) afforded complex **4** as colorless crystals in 38% yield (0.180 g). Protocol B: HOC(CF$_3$)$_3$ (0.405 g, 0.24 mL, 1.71 mmol) was condensed to a solution of Tb(CH$_2$C$_6$H$_4$NMe$_2$-*o*)$_3$ (0.320 g, 0.57 mmol) in THF (40 mL). The reaction mixture was stirred overnight at ambient temperature. All volatiles were removed in vacuum. The reaction product was dissolved in 3 mL of THF. Slow condensation of hexane to a resulted THF solution (2:1 ratio) afforded **4** as colourless crystals in 76% yield (0.460 g). Elemental analysis calc. for C$_{24}$H$_{24}$F$_{27}$O$_6$Tb (1080.33 g·mol^{-1}) (%): C, 26.86; H, 2.24; Tb, 14.71. Found (%): C, 26.77; H, 2.39; Tb, 14.85. IR (Nujol, KBr) ν/cm^{-1}: 1700 (m), 1612 (m), 1578 (m), 1323 (s), 1299 (s), 1272 (s), 1245 (s), 1215 (s), 1195 (s), 1159 (s), 1100 (m), 1019 (s), 967 (s), 927 (m), 915 (m), 873 (s), 841 (s), 803 (m), 773 (m), 708 (s), 672 (m), 627 (w), 613 (s), 604 (w), 568 (w), 537 (w) (Figure S5, ESI).

X-ray crystallography

X-ray diffraction data for **1–4** were collected at 100 K with a Bruker Quest D8 CMOS diffractometer, using graphite monochromated Mo-K_α radiation (λ = 0.71073 Å, ω-scans). Structures were solved using Intrinsic Phasing with the ShelXT [5] structure solution program in Olex2 [6] and then refined with the XL [7] refinement package using Least-Squares minimization against F^2 in the anisotropic approximation for non-hydrogen atoms. Positions of hydrogen atoms were calculated, and they were refined in the isotropic approximation within the riding model. Disordered lattice molecules of THF in **1** and **2** were treated as diffuse contributions to the overall scattering without specific atom positions using the Solvent Mask routine implemented in OLEX2. Main structural parameters for **1**–**4** are given in Table S1. Crystal data and structure refinement parameters are given in Table S3. CCDC 2206279 (**1**), 2206278 (**2**), 2206277 (**3**), and 2206602 (**4**) contain the supplementary crystallographic data for this paper.

Photoluminescence spectra

Luminescence excitation spectra and luminescence decays were obtained using a Horiba Fluorolog QM spectrofluorometer with a 75 W xenon arc lamp as excitation source and a R13456 (Hamamatsu, Japan) photomultiplier tube sensitive in the 200–980 nm spectral range as a detector. The absolute quantum yields (PLQYs, Φ) were measured using a Spectralon-covered G8 integration sphere (GMP SA, Switzerland) coupled to the spectrofluorometer. According to our estimates, the consistent experimental error of measuring the quantum yields did not to exceed 15%. For low-temperature experiments samples were placed in quartz tubes of 5 mm o.d. inserted in a quartz Dewar-type cryostat filled with liquid nitrogen at 77 K. For kinetic measurements xenon flash lamp was used as an excitation source.

Magnetism

Magnetic susceptibility data were collected with a Quantum Design MPMS-XL SQUID magnetometer working between 1.8–350 K with the magnetic field up to 7 Tesla. The samples were prepared in in glow box. The data were corrected for the sample holder and the diamagnetic contributions calculated from the Pascal's constants.

References:

S1 M. D. Taylor and C. P. Carter, *J. Inorg. Nucl. Chem.*, 1962, **24**, 387; https://doi.org/10.1016/0022-1902(62)80034-7.

S2 J. T. B. H. Jastrzebski, G. V. Koten, M. F. Lappert, P. C. Blake and D. R. Hankey, Cyclometallated Organolithium Compounds. In *Inorganic Syntheses*; John Wiley & Sons, Ltd, 1989; pp. 150–155 ISBN 978-0-470-13257-9.

S3 D. M. Amorose, R. A. Lee and J. L. Petersen, *Organometallics*, 1991, **10**, 2191; https://doi.org/10.1021/om00053a023.

S4 S. J. Lyle and Md. M. Rahman, *Talanta*, 1963, **10**, 1177; https://doi.org/10.1016/0039-9140(63)80170-8.

S5 G. M. Sheldrick, *Acta Cryst A*, 2015, **71**, 3; https://doi.org/10.1107/S2053273314026370.

S6 O. V. Dolomanov, L. J. Bourhis, R. J. Gildea, J. K. Howard, H. Puschmann, *J Appl Cryst*., 2009, **42**, 339; https://doi.org/10.1107/S0021889808042726.

S7 G. M. Sheldrick, *Acta Cryst A*, 2008, **64**, 112; https://doi.org/10.1107/S0108767307043930.

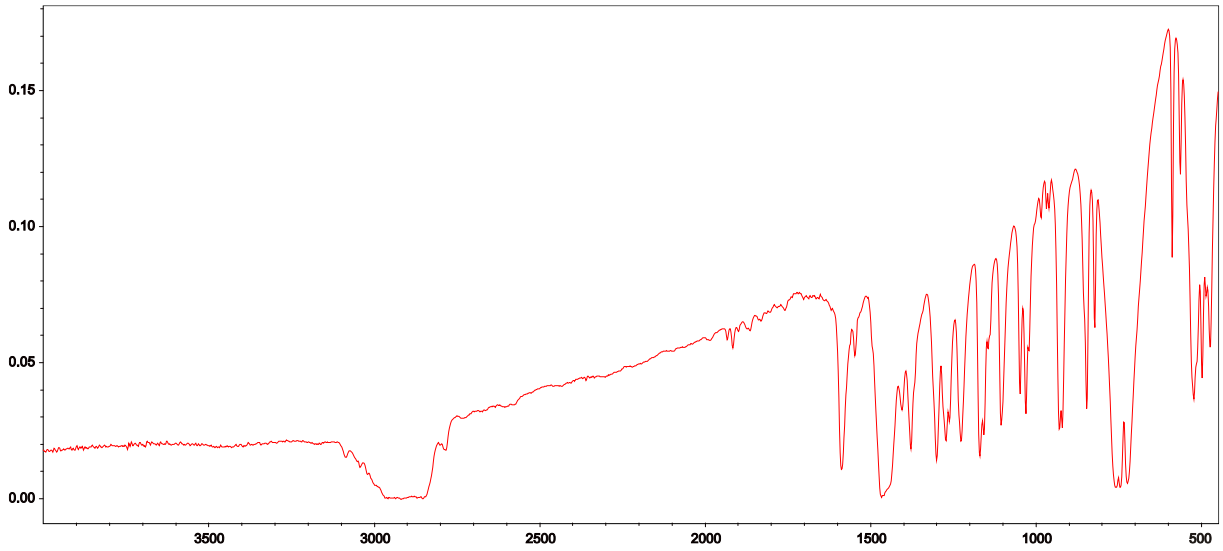

Figure S1. IR spectrum of $Tb(CH_2C_6H_4NMe_2\text{-}o)_3$ (Nujol, KBr).

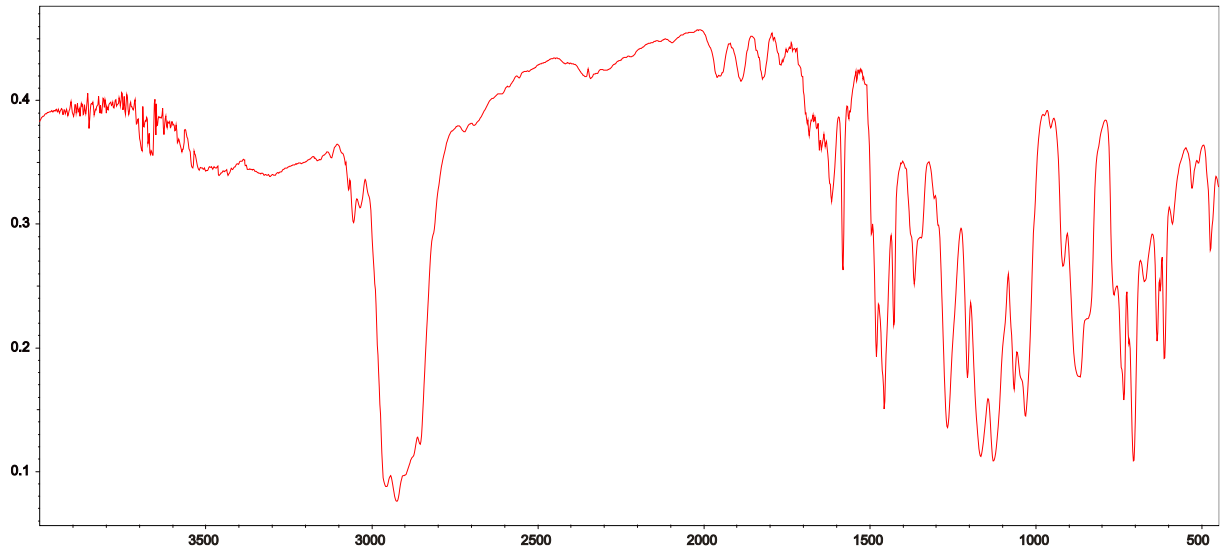

Figure S2. IR spectrum of **1** (Nujol, KBr).

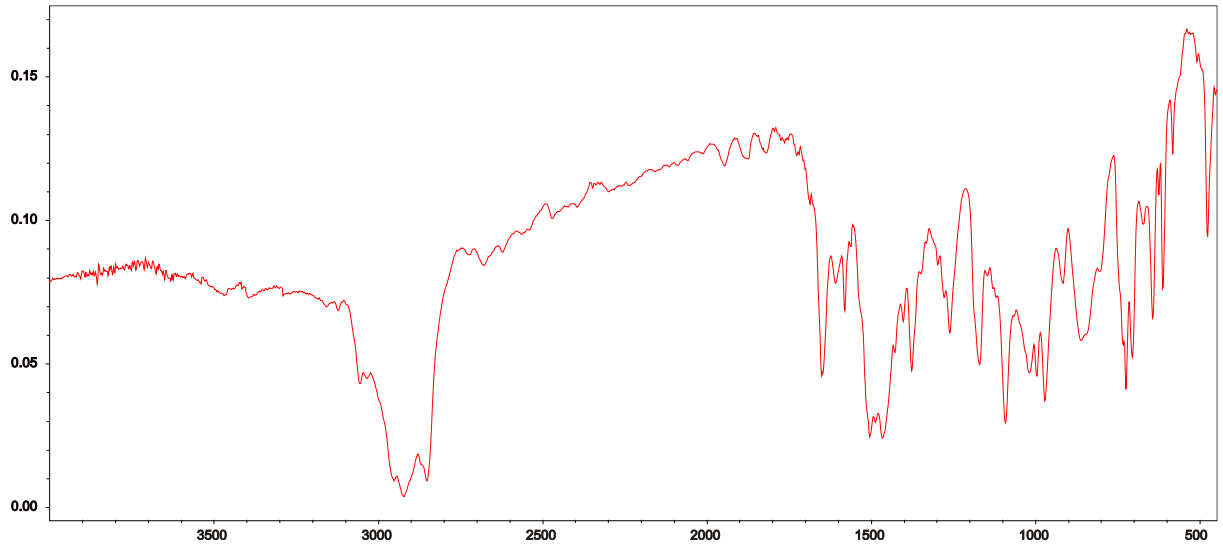

Figure S3. IR spectrum of **2** (Nujol, KBr).

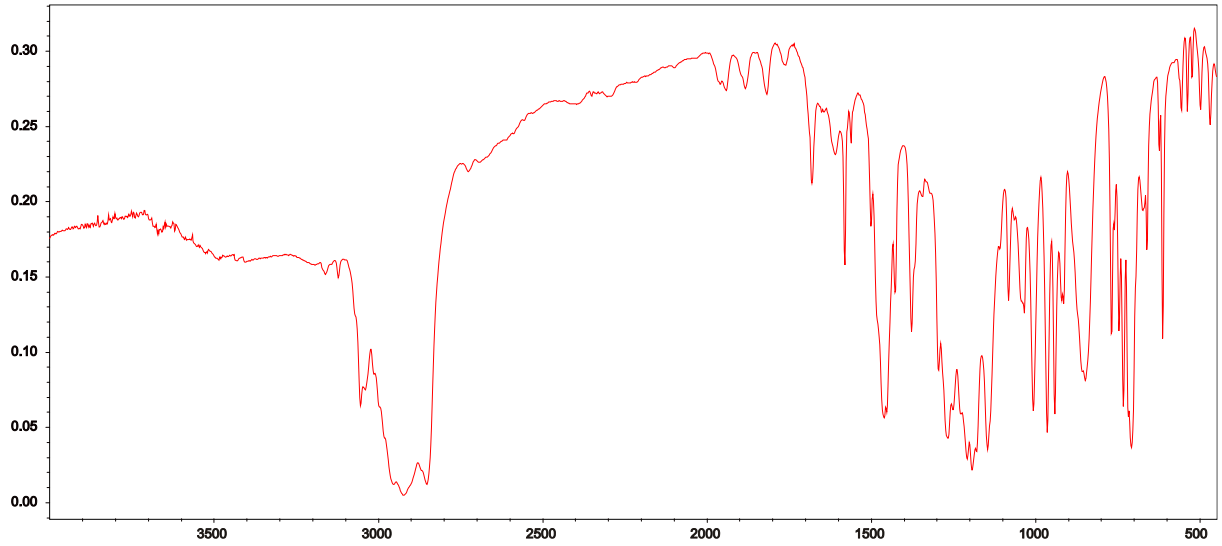

Figure S4. IR spectrum of **3** (Nujol, KBr).

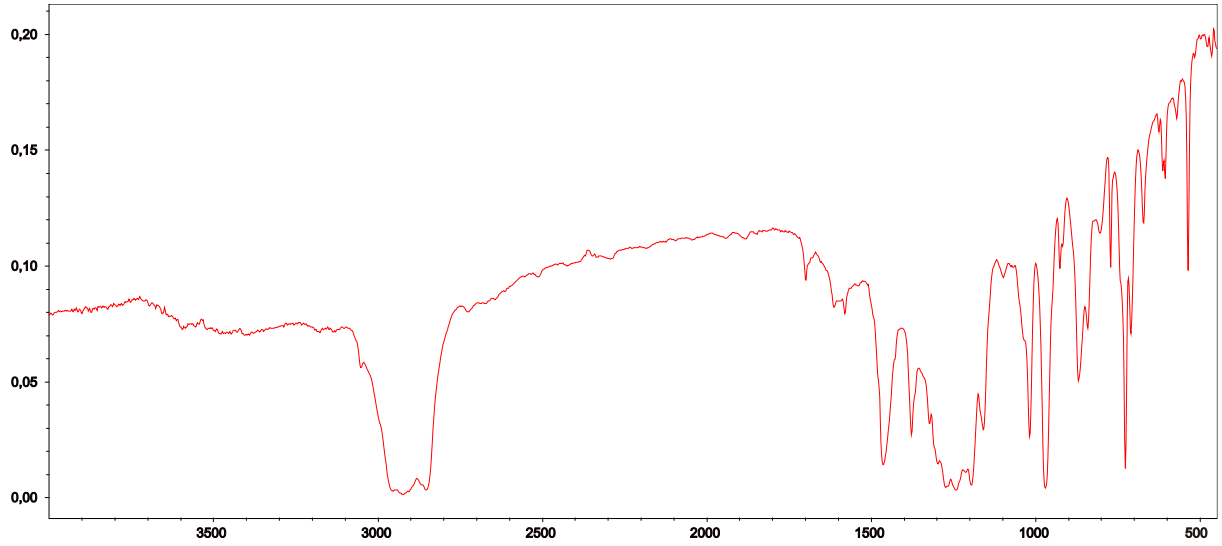

Figure S5. IR spectrum of **4** (Nujol, KBr).

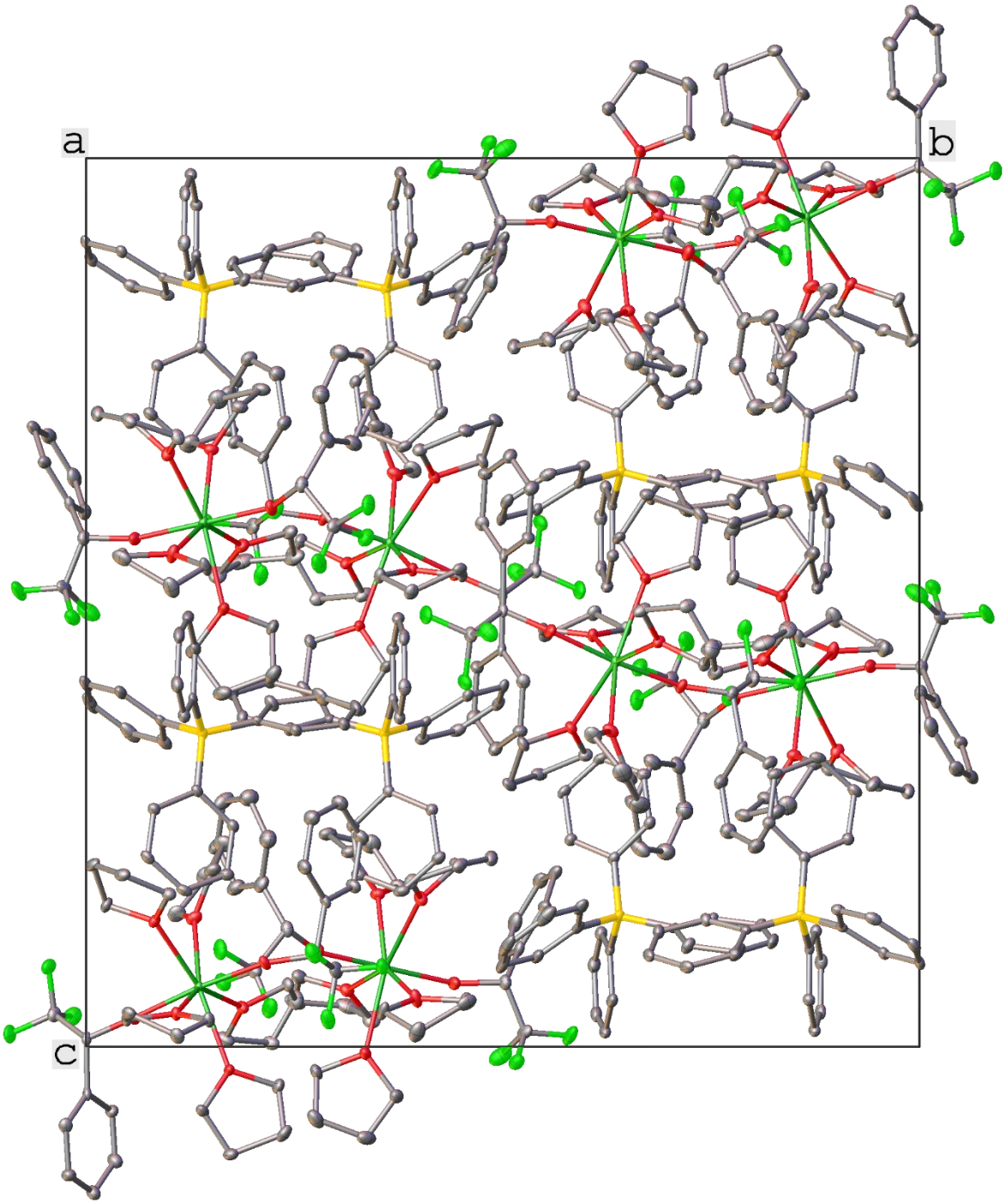

Figure S6. Perspective view of the crystal packing for **1** along the crystallographic axis *a*. Hydrogen atoms and minor components of the disordered ligands have been omitted for clarity. Color code: green Tb; light green F; red O; grey C; yellow B.

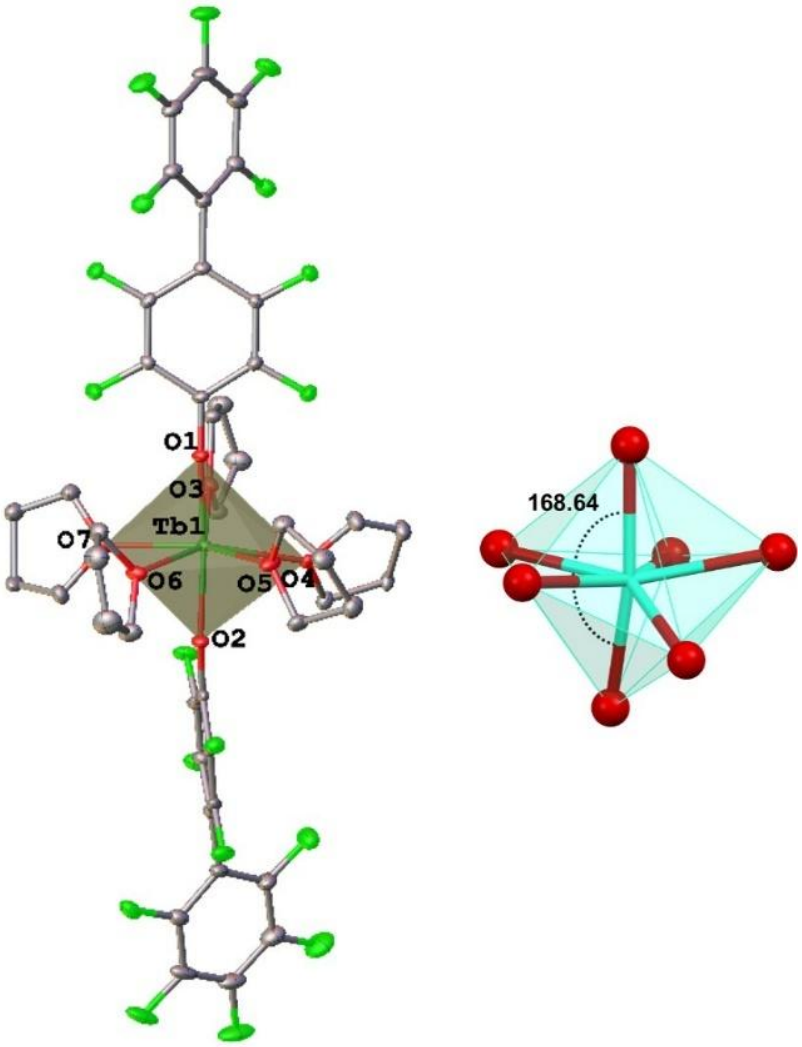

Figure S7. (left) General view of the cationic complex **2** showing the coordination environment of the Tb^{3+} ion; (right) Coordination polyhedron of Tb^{3+} in **2**.

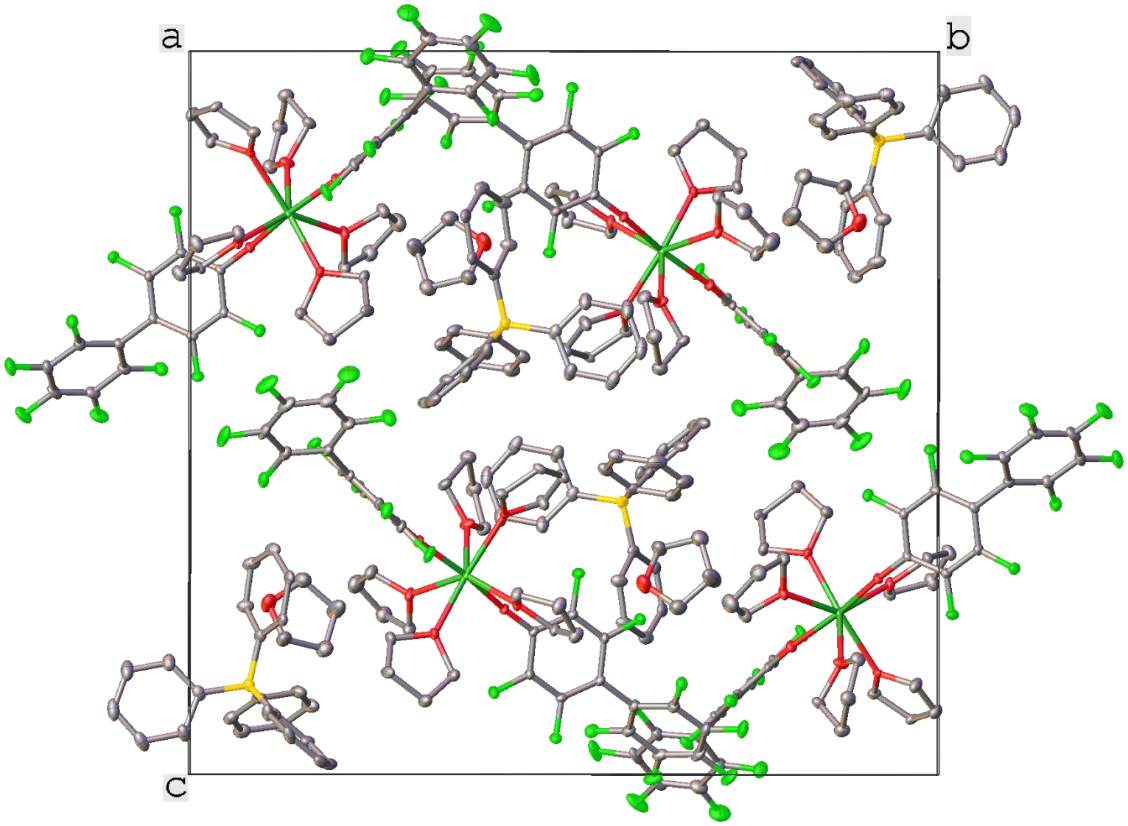

Figure S8. Perspective view of the crystal packing for **2** along the crystallographic axis *a*. Hydrogen atoms are been omitted for clarity. Color code: green Tb; light green F; red O; grey C; yellow B.

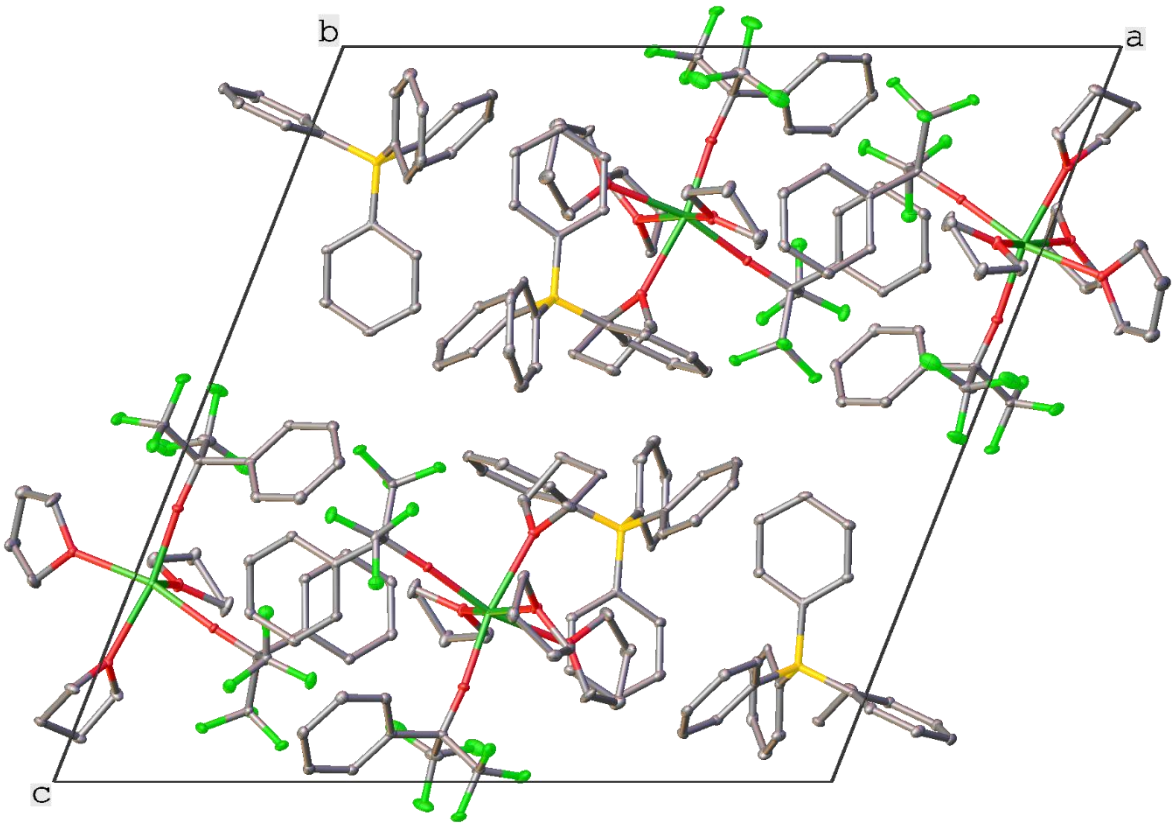

Figure S9. Perspective view of the crystal packing for **3** along the crystallographic axis *b*. Hydrogen atoms are omitted for clarity. Color code: green Tb; light green F; red O; grey C; yellow B.

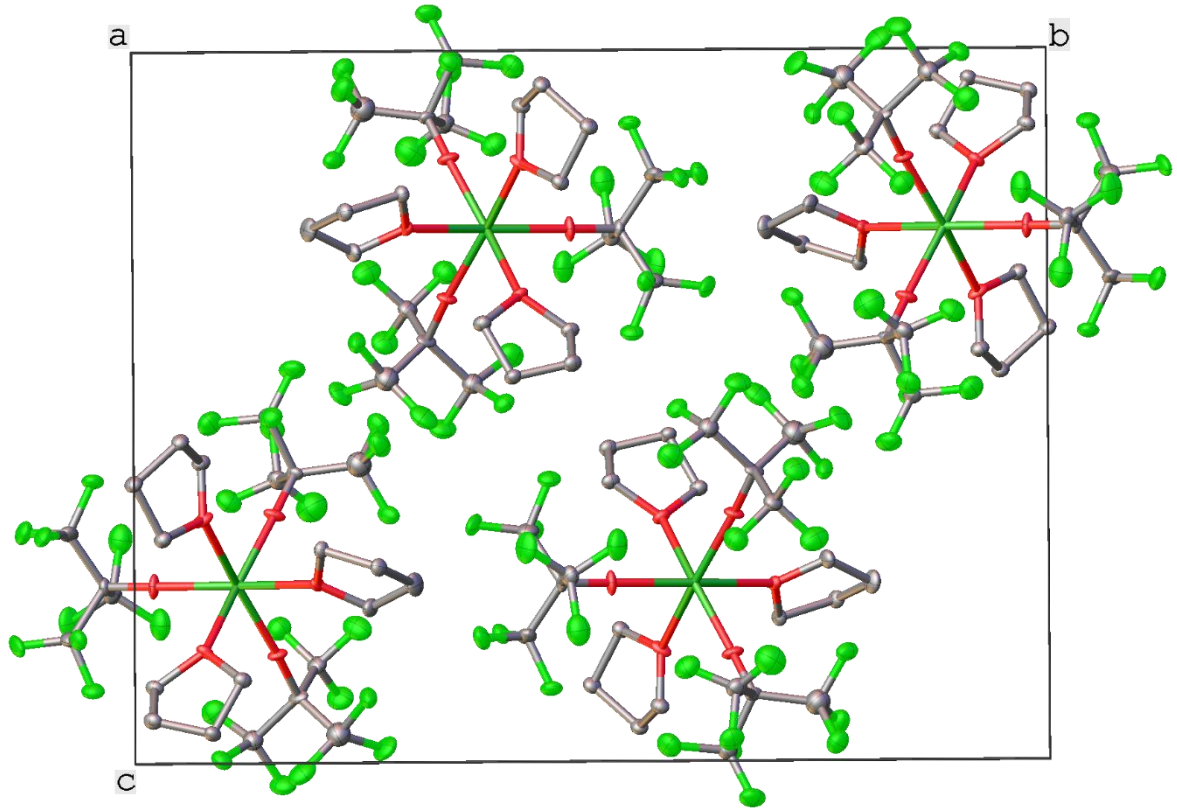

Figure S10. Perspective view of the crystal packing for **4** along the crystallographic axis *a*. Hydrogen atoms are omitted for clarity. Color code: green Tb; light green F; red O; grey C; yellow B.

Table S1. Main structural parameters for **1**–**4**.

Compound		Tb−OR distances (Å)	Tb−O (THF) distances (Å)	Axial O−Tb−O angle (°)
1	**1a**	2.123(2) 2.126(2)	2.403(2)–2.473(2)	177.75(11)
	1b	2.119(2) 2.119(2)	2.408(2)–2.476(3)	174.07(10)
2		2.160(2) 2.167(2)	2.392(3)–2.421(3)	168.64(10)°
3		2.117(2) 2.107(2)	2.331(2)–2.423(2)	164.86(10)–169.72(8)
4		2.143(6) 2.137(6) 2.132(6)	2.411(6)–2.428(6)	163.6(2)–165.4(2)

Magnetic properties

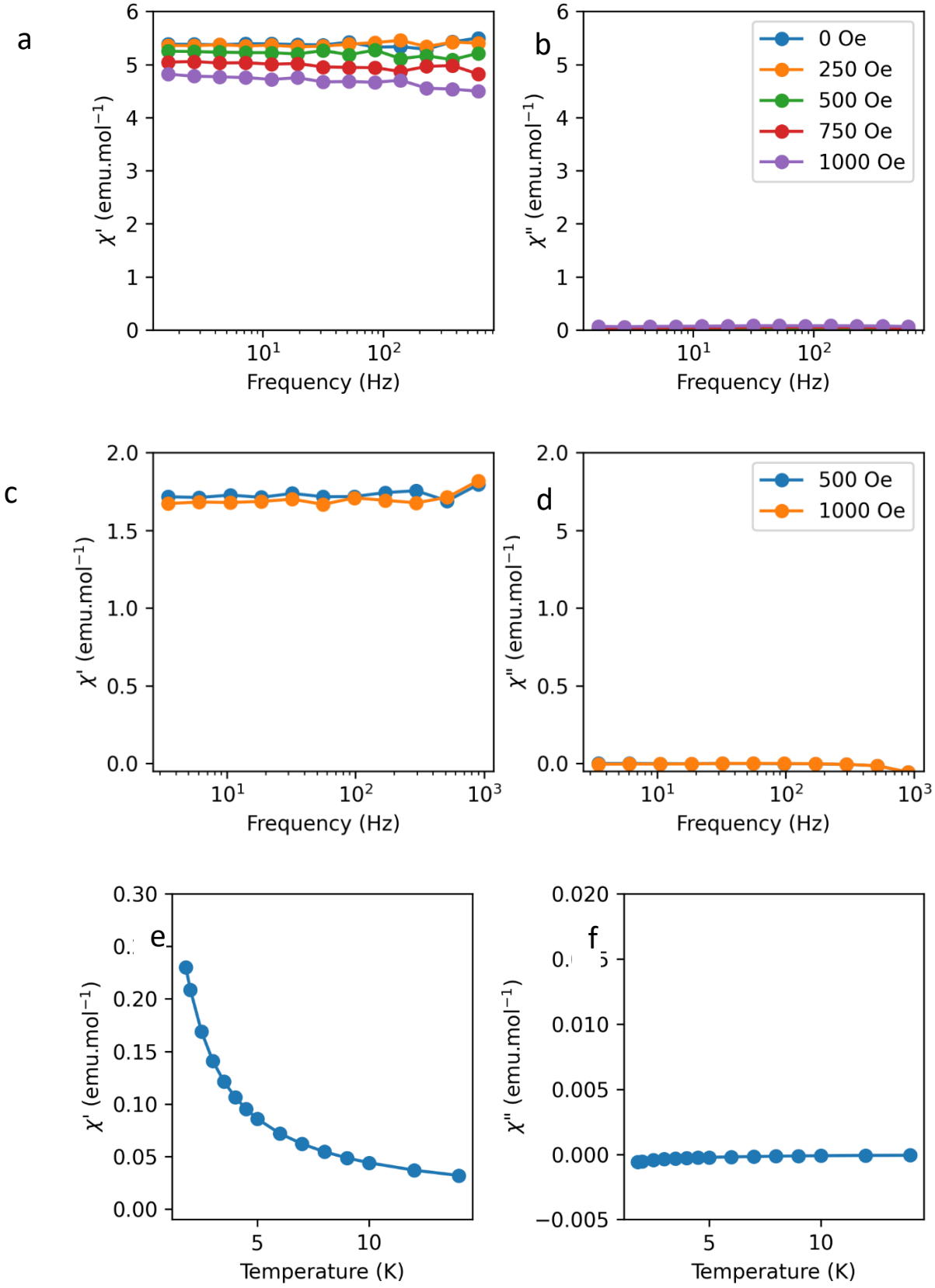

Figure S11. Frequency dependence of χ' (a) and χ'' (b) components of the ac susceptibility performed for sample **2** at 1.8 K with different applied fields (200 Oe (blue), 500 Oe (orange), 1200 Oe (green), 2500 Oe (red), 3500 Oe (violet)); Frequency dependence of χ' (c) and χ'' (d) components of the ac susceptibility performed for sample **3** at 1.8 K with different applied fields (1000 Oe (blue), 2500 Oe (orange)); Temperature dependence of χ' (e) and χ'' (f) components of the ac susceptibility performed for sample **4** at 125 Hz under 1500 Oe applied field.

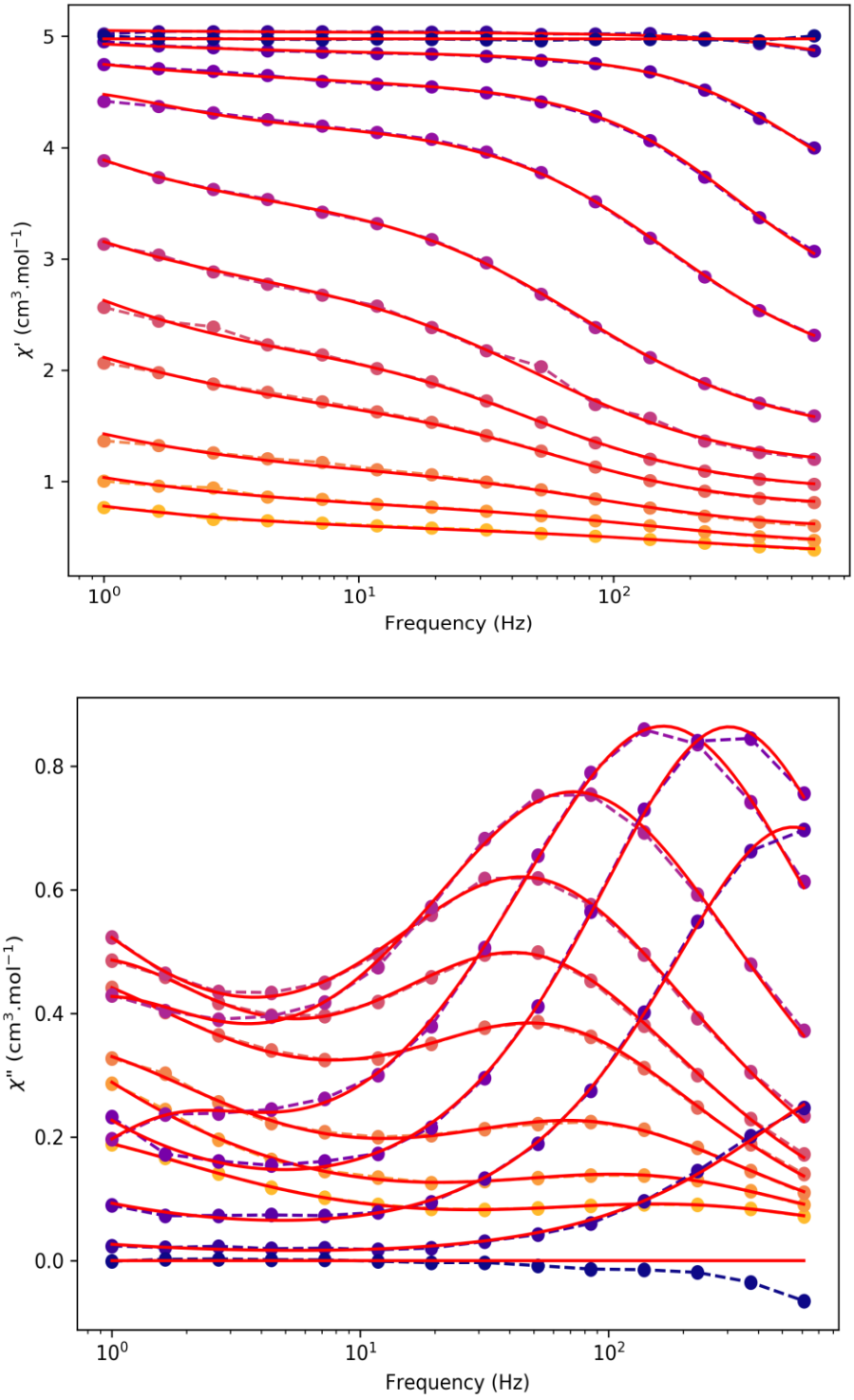

Figure S12. Frequency dependence of χ' (top) and χ'' (bottom) for **1** at 1.8 K performed under various dc fields.

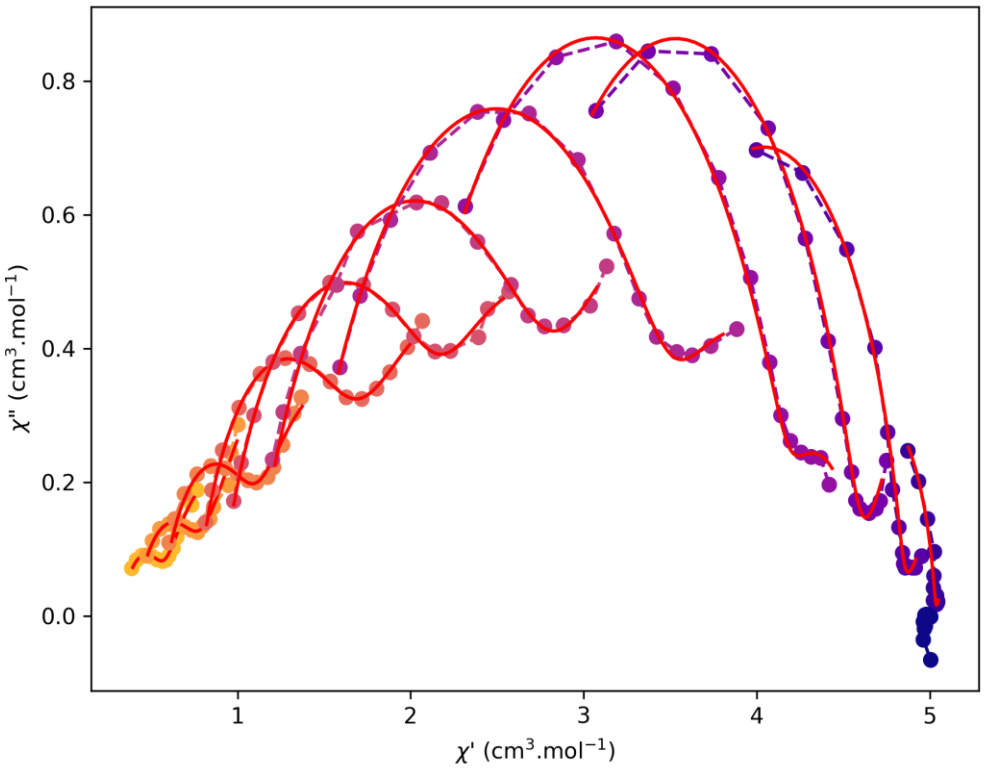

Figure S13. Cole-Cole plots obtained using the frequency dependence of χ'' for **1** at 1.8 K under various dc field. The solid lines correspond to the best fit obtained with a generalized Debye model.

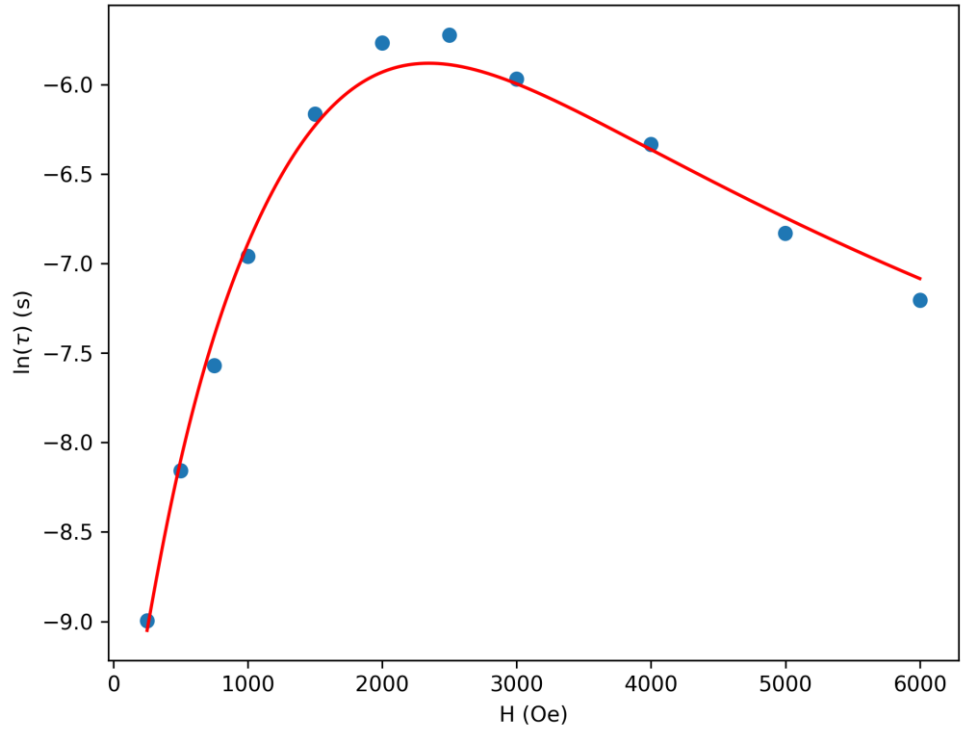

Figure S14. Field dependence of the relaxation time curve for **1**. The solid lines correspond to the best fit obtained with eq. $\boldsymbol{\tau^{-1} = D \cdot H^2 \cdot T + \frac{B_1}{1+B_2 \cdot H^2}}$.

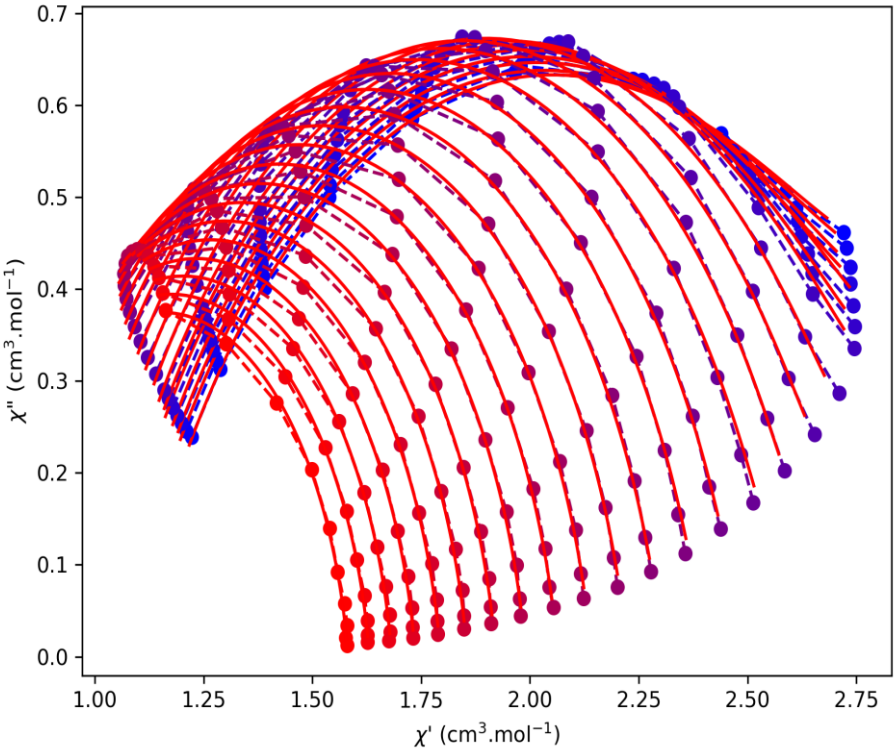

Figure S15. Cole-Cole plots obtained using the frequency dependence of χ'' for **1** obtained under 2000 Oe. The solid lines correspond to the best fit obtained with a generalized Debye model.

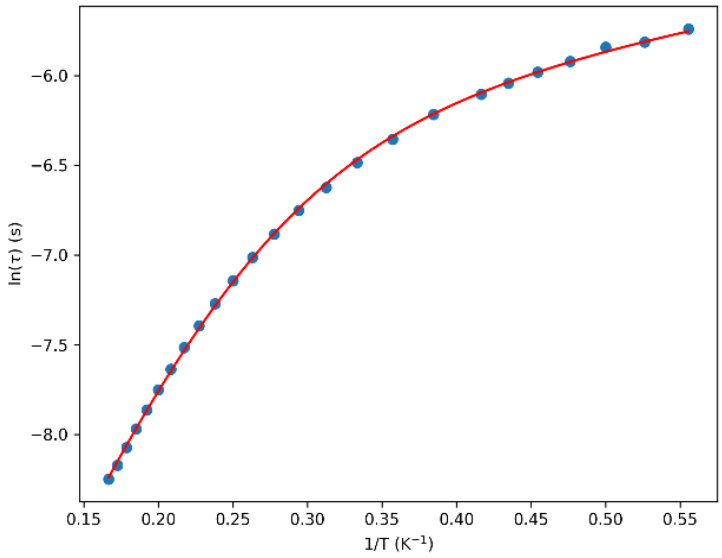

Figure S16. The relaxation time as a function of temperature for **1** under the optimal magnetic field of 2000 Oe (blue points) and the corresponding fit with Eq. 2 (red solid line).

Photoluminescence properties

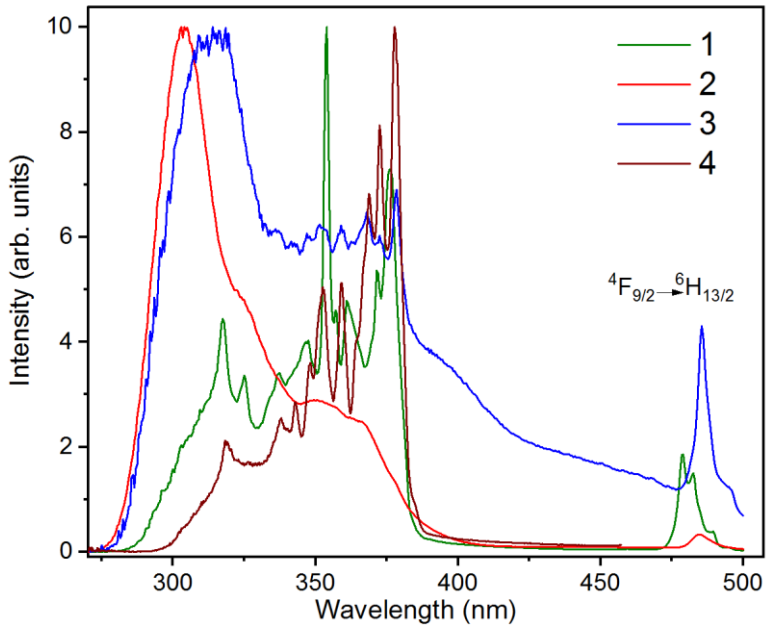

Figure S17. Excitation spectra of the compounds **1 - 4** monitored at λ_{em} = 543 nm at 77 K.

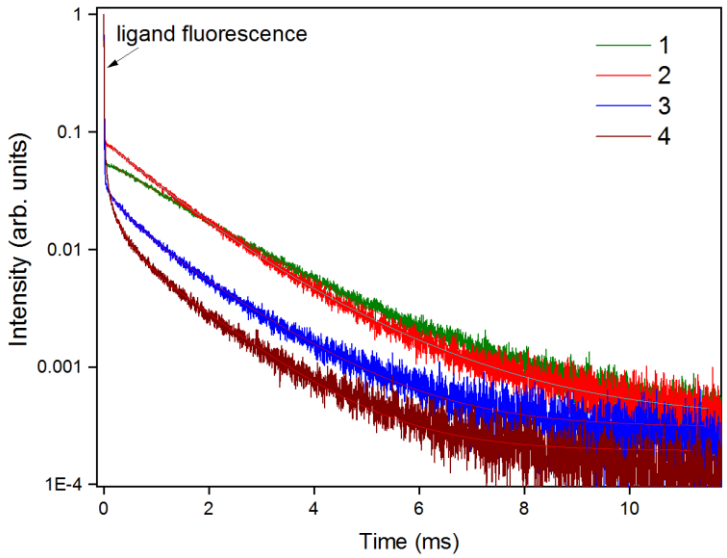

Figure S18. Photoluminescent decays for the compounds **1**–**4** under excitation at 310 nm at room temperature.

Table S2. Photophysical parameters for **1**–**4**.

Complex	τ_1, μs	τ_2, μs	A_1/A_2	R^2	Φ, %
1	1668±0.9	-	3.0	0.998	2
2	1010±9	2048±15	0.95	0.999	11
3	452±5	1467±6	0.74	0.998	6
4	270±2	1291±4	1.50	0.996	1

Table S3: Crystal data, data collection and structure refinement details for **1**–**4**.

Identification code	**1**	**2**	**3**	**4**
Empirical formula	$C_{60}H_{72}BF_6O_7Tb$	$C_{72}H_{68}BF_{18}O_8Tb$	$C_{58}H_{62}BF_{12}O_6Tb$	$C_{24}H_{24}F_{27}O_6Tb$
Formula weight	1188.90	1572.99	1252.80	1080.35
Temperature, K	100	100	100	100
Crystal system	Monoclinic	Monoclinic	Monoclinic	Monoclinic
Space group	$P2_1/n$	$P2_1/c$	$P2_1/n$	$P2_1/n$
a, Å	20.4447(4)	12.8917(5)	20.3100(3)	9.7005(2)
b, Å	23.0013(4)	24.1412(8)	13.8765(2)	21.5239(6)
c, Å	24.7175(4)	23.3340(8)	20.6184(3)	16.7469(4)
α, deg.	90	90	90	90
β, deg.	96.7400(10)	92.400(2)	111.4950(10)	90.2600(10)
γ, deg.	90	90	90	90
V, Å^3	11543.2(4)	7255.7(4)	5406.77(14)	3496.59(15)
Z	8	4	4	4
Density (calc.), g/cm^3	1.368	1.440	1.539	2.052
Absorption coefficient, mm^{-1}	12.94	10.73	14	22.05
F(000)	4896	3184	2544	2096
Theta range, deg.	54	54	56	52
Reflections collected	132510	82936	66630	35492
Independent reflections, R_{int}	25203	15846	13064	6873
Reflections with $I > 2\sigma(I)$	19101	12221	9568	6011
Parameters refined	1439	969	703	662
Goodness-of-fit on F^2	1.010	1.023	1.019	1.050
R_1 / wR_2 for $I > 2\sigma(I)$	0.0382/0.0768	0.0426/0.1010	0.0372/0.0774	0.0652/0.0723
R_1 / wR_2 for all data	0.0589/0.0854	0.0602/0.1106	0.0594/0.0867	0.1588/0.1645
$\Delta\rho_{max}$ / $\Delta\rho_{min}$, e·Å^{-3}	0.771/−0.850	0.865/−0.602	1.854/−0.851	1.965/−1.379